Surface Science 282 (1993) 357–370
North-Holland

surface science

Dry etching of GaAs with Cl_2: correlation between the surface Cl coverage and the etching rate at steady state

Chaochin Su, Ming Xi, Zi-Guo Dai, Matthew F. Vernon and Brian E. Bent *
Department of Chemistry, Columbia University, New York, NY 10027, USA

Received 29 September 1992; accepted for publication 3 November 1992

While dry etching of GaAs with chlorine is technologically important for manufacturing semiconductor devices, little is known conclusively about the surface chemical reactivity responsible for this etching process. In this work, modulated molecular beam scattering (MMBS) has been combined with temperature-programmed reaction (TPR) and Auger electron spectroscopy (AES) to study the reaction of molecular chlorine with GaAs. The MMBS and AES results indicate that the surface coverage of chlorine during steady state etching over the temperature range of 350–650 K is in the monolayer regime. Above 700 K the surface is chlorine free. A direct correlation is observed between the number of vacant surface sites and the Cl_2 reaction probability. This result suggests a Langmuir adsorption model for the surface reaction, and it is shown that such a model combined with the product evolution kinetics determined from TPR studies successfully simulates the temperature dependence of the chlorine evolved from the surface during modulated molecular beam scattering.

1. Introduction

Dry etching of GaAs surfaces by Cl_2 is an important process for the manufacture of GaAs-based microelectronics devices [1]. Despite numerous recent studies of the thermal [1–14] as well as ion- [1,4,15–18], electron- [19,20], and photo-assisted [10,21,22] process, the molecular basis for these processes has yet to be established. Among the important issues are the etching products, the rate-limiting steps, and the nature of the potentially corrosive chlorinated layer present on the surface during processing. We have recently addressed these questions for the thermal etching process. In previous papers [7,8], the reaction products and absolute etching rate as a function of surface temperature and Cl_2 flux have been established. In the present work, modulated molecular beam scattering (MMBS), temperature-programmed reaction (TPR) studies, and in situ Auger electron spectroscopy (AES) have been applied to establish a quantitative correlation between the surface chlorine coverage and the thermal etching rate at steady state.

The bonding of chlorine to GaAs surfaces under vacuum conditions has been addressed previously by a number of investors [23,24]. There is evidence that, below room temperature where there is no detectable etching, chlorine penetrates into GaAs to form a chlorinated layer which can reach a depth of up to 40 Å [25]. Thicker layers can be formed if the surface is exposed to Cl atoms as opposed to Cl_2 [25]. At room temperature, the surface chlorine coverage is in the monolayer regime, and submonolayers of chlorine remain adsorbed on the surface up to 573 K [14,25]. Despite several XPS studies [2,14,23,25,26], there is still controversy over whether chlorine bonds to Ga and/or As over the 273–573 K temperature range, and it appears likely that the surface bonding varies depending on whether Ga- or As-rich surfaces are prepared. A recent series of elegant temperature-programmed desorption (TPD) and metastable quenching spectroscopy (MQS) studies by Lud-

* To whom correspondence should be addressed.

viksson et al. strongly suggest that on the Ga-rich c(8 × 2) surface, chlorine bonds to Ga up to 550 K where GaCl is evolved from the surface [24]. On rougher surfaces, there is evidence that a $GaCl_2$ species can also be formed below 250 K [24]. TPR studies by a number of groups [9,24] have shown that $AsCl_3$ forms and desorbs from an As-rich GaAs(100) at temperatures below 200 K leaving behind a $GaCl_x$ matrix ($x = 1$–3). $GaCl_3$ and $GaCl_2$ evolution are subsequently observed at 250–400 K [9,15,24], while GaCl desorbs at 500–650 K [9,15,24,27]. The high temperature As-products are As_4 and As_2 [9,24].

In all the studies described above, the chlorinated GaAs surfaces were investigated under vacuum conditions in the absence of any Cl_2 flux. In the present work, the surface chlorine coverage in situ is quantified by combining modulated molecular beam scattering experiments with temperature-programmed reaction studies. An important finding is that the chlorine coverage is in the monolayer regime over the temperature range of 350–650 K, and that above this temperature, the surface is chlorine-free. At temperatures where the reaction is not reactant flux-limited, the steady state etching rate is directly proportional to the number of vacant sites in the chlorine monolayer. The Langmuir nature of the steady state etching reaction is confirmed by Auger electron spectroscopy measurements of the surface chlorine coverage during etching under low reactant flux conditions in an ultra-high vacuum (UHV) apparatus.

2. Experimental

The surface Cl coverage during the Cl_2 + GaAs etching reaction was studied by a combination of modulated molecular beam scattering (MMBS), temperature-programmed reaction (TPR), and Auger electron spectroscopy (AES). The MMBS and TPR experiments were performed in a modified crossed molecular beam machine. The essential features of this apparatus can be found in previous publications [7,8]. The experimental methods and analysis procedures have also been described elsewhere [8,28]. Briefly, in the MMBS experiments, a GaAs wafer is etched by a modulated Cl_2 beam and the products that are evolved from the surface are detected by a quadrupole mass spectrometer (QMS). In the studies reported here, the GaAs wafers (undoped with a nominal (100) orientation) were mounted on a resistive heating element for temperature control between 350 and 900 K. The wafers were precleaned with chloroform, acetone, bromine/methanol, methanol and then etched in situ with Cl_2 at 800 K. Numerous prior experiments have shown that this procedure produces a surface which gives reproducible etching results [8]. In addition, as discussed in section 3, the results of AES studies on Cl/GaAs(100) prepared under ultra-high vacuum conditions are consistent with the surface Cl coverages determined by MMBS in this molecular beam system.

The modulated molecular beam scattering experiments were carried out by expanding a 5% Cl_2 in He mixture from a stagnation pressure of 200 Torr through a graphite nozzle (0.127 mm diameter aperture) into vacuum. The beam is collimated to a 6° divergence by a conical graphite skimmer; a mechanical shutter further collimates the beam to 0.7° divergence and chops the beam to produce gas pulses from 0.1 ms to 1000 s in duration. The Cl_2 molecules impinge onto the GaAs surface at 65° from the surface normal, and the etching products evolved are detected with the QMS oriented at 30° from the surface normal in the plane defined by the incident Cl_2 beam and the surface normal. The modulation waveforms presented in this work are typically the sum of 2 sequential modulation cycles at high surface temperature and of 16 sequential modulation cycles at low surface temperature. Studies with a Cl_2/Ar beam suggest that the higher than thermal kinetic energy of the Cl_2 in the supersonic Cl_2/He beam does not have a substantial effect on the results presented here [8]. The specific effects of translational energy on the dissociation and scattering of Cl_2 from GaAs(110) have been thoroughly investigated by DeLouise [3].

An important parameter in the experiments here is the Cl_2 flux. Based on the experimental configuration and the principles of gas dynamics [29], the calculated Cl_2 flux incident on the sur-

face is 5.5×10^{15} molecules/cm^2/s. Two independent checks suggest that this value is accurate to within at least an order of magnitude. First, we have previously utilized measurements of the As_2 flux during GaAs evaporation and Cl_2 etching together with a Cl_2 mass balance to calibrate the Cl_2 flux relative to the reported evaporation rate for GaAs(100) in the literature [8,30]. This yields a Cl_2 flux of 2.8 monolayers (ML)/s (1.75×10^{15} molecules/cm^2/s), with the uncertainties being the degree of surface roughness and the sensitivity of the evaporation rate to the method of surface preparation [31]. In the present work, we have used the GaCl TPR spectra from a Ga-rich surface as a calibration point for the Cl_2 flux. In particular, recent results from Ludviksson et al. [24] suggest that the amount of GaCl desorbed from a saturated monolayer on the Ga-rich c(2 × 8) GaAs(100) surface is $\theta = 0.75$ (number of GaCl per surface atom for a surface atomic density of 6.25×10^{14} molecules/cm^2). Assuming this value, we use the GaCl TPR spectrum in fig. 5B to calibrate the $GaCl^+$ ion intensity. We then apply a Cl mass balance on the steady state etching products as described in ref. [8] and obtain a Cl_2 flux of 1.2 ML/s (7.5×10^{14} molecules/cm^2/s). This value is the one used in the studies reported here.

The TPR experiments were carried out in the same apparatus as the MMBS studies. Chlorine was adsorbed onto the GaAs surface at 340 K from the molecular beam source, and the surface was heated at 1 K/s while monitoring the desorbing species. Up to nine masses were monitored simultaneously. After verifying from the cracking patterns that the desorbing products are $GaCl_3$, GaCl, Ga, $AsCl_3$, As_2 and As_4 consistent with our previous reports on the steady state etching [7,8], we have followed only the following nine masses: 70 ($^{35}Cl_2$), 104 ($^{69}Ga^{35}Cl$), 110 ($^{75}As^{35}Cl$), 141 ($^{69}Ga^{35}Cl^{37}Cl$ and $^{71}Ga^{35}Cl_2$), 150 ($^{75}As_2$), 176 ($^{69}Ga^{35}Cl_2{}^{37}Cl$ and $^{71}Ga^{35}Cl_3$), 182 ($^{75}As^{35}Cl_2{}^{37}Cl$), 225 ($^{75}As_3$), and 300 ($^{75}As_4$). Between each TPR experiment, a blank TPR spectrum was acquired to determine the contributions from the background.

The Auger electron spectroscopy experiments were executed in an ion- and titanium sublimation-pumped UHV chamber which has been previously described [32]. In brief, the system is equipped with capabilities for low-energy electron diffraction (LEED), AES, ion sputtering, and TPR experiments. A base pressure of 2×10^{-10} Torr was routinely achieved. The GaAs surface was cleaned by Ar^+ sputtering (500 eV) at 300 K followed by annealing at 700 K. This procedure produces a gallium-rich surface. Because of extensive steady state chlorine etching, however, the surfaces were roughened [8]; electron diffraction was observed from these surfaces, but the spots were not sharp or indexable.

To study the Cl coverage on the surface, Cl_2 was adsorbed onto the crystal at 110 K by backfilling the chamber, and AES spectra were recorded immediately after reaching the desired surface temperature. Exposures are reported in langmuirs (1 langmuir = 1×10^{-6} Torr · s), L, and are uncorrected for different ion gauge sensitivities. Between each experiment, a clean and reproducible surface was confirmed by AES.

An experimental complication in the AES measurements on the Cl_2/GaAs system is that the ^{181}Cl peak intensity decreases during the measurement. The apparent reason is electron-stimulated desorption (ESD) of chlorine which has been reported previously by Mokler et al. [19]. To quantify this effect, we have carefully monitored the ^{181}Cl Auger intensity as a function

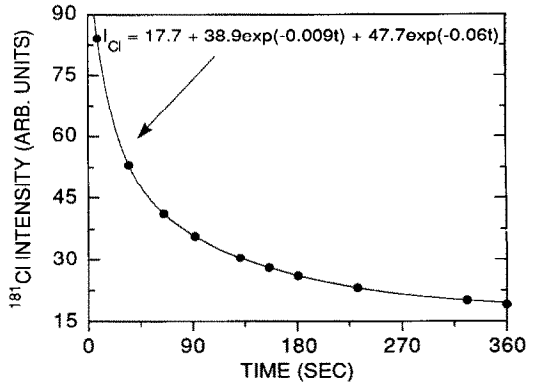

Fig. 1. The effect of electron exposure on the ^{181}Cl Auger signal from chlorine adsorbed on GaAs(100). The experimental conditions are described in the text. The solid line is a bi-exponential fit to the electron stimulated desorption process.

of electron exposure. The spectra were acquired using a single pass cylindrical mirror analyzer (CMA) with a modulation amplitude of 3 eV. The surface atoms were ionized by a 3 keV electron beam incident on surface at normal incidence, and the current to ground during these experiments was ~ 1 mA. Fig. 1 shows the ^{181}Cl Auger peak intensity as a function of electron beam exposure after dosing 2L of Cl_2 at 116 K. Clearly, the adsorbed Cl on GaAs(100) is very sensitive to ESD under this condition. The ratio of the Auger peak intensity for ^{181}Cl to ^{1070}Ga is 1.5 after 8 seconds of electron beam exposure. Moreover, as shown in fig. 1, the ^{181}Cl signal decay due to ESD is well-fit by a double exponential function. All the Auger peak intensities reported in this paper have been corrected using such a bi-exponential function.

3. Results and interpretation

In presenting the results on the correlation between the surface Cl coverage and the steady state etching rate for the Cl_2 + GaAs reaction, we begin first with a summary of previous results on the etching products and etching rate at steady state [8,28]. We then present the results of MMBS and TPR studies from which the chlorine evolved from the surface under steady state and non-steady state etching conditions is derived. Finally, the temperature dependence of the surface Cl coverage determined from AES measurements is reported.

3.1. Etching products and rate at steady state

The products and rate of the thermal etching of GaAs by Cl_2 at steady state have been investigated previously [8] and the results are summarized in fig. 2. Three important conclusions are evident. Firstly, as shown in fig. 2A, the predominant etching products and the temperature ranges over which they are evolved are: $GaCl_3$ (350–700 K), GaCl (600–950 K), Ga (> 850 K), $AsCl_3$ (350–550 K), As_2 (650–950 K) and As_4 (400–850 K). Secondly, as shown in fig. 2B, with appropriate choices for the mass spectrometric detection

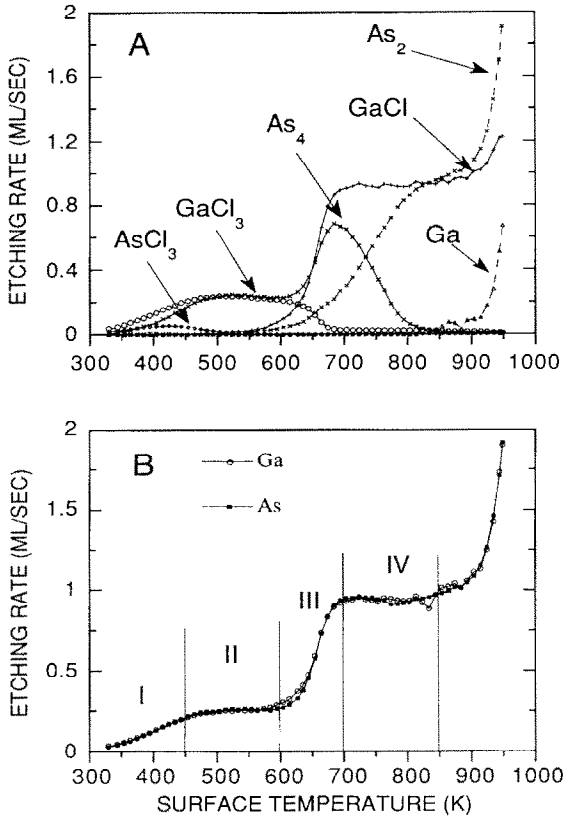

Fig. 2. Surface temperature dependence of (A) the etching rates attributable to the indicated product fluxes and (B) the absolute etching rate of Ga (open circles) and As (solid squares) for the $GaAs/Cl_2$ reaction [8]. Note that the As_4 and As_2 *fluxes* are factors of 4 and 2, respectively, less than the *etching rates* shown. The Cl_2 flux in these experiments was ~ 7.5×10^{14} $Cl_2/cm^2/s$.

sensitivity factors for these six products, the bulk Ga:As stoichiometry (1:1) is reproduced over the entire temperature range studied. Thirdly, the etching rate with respect to surface temperature (T_s) shows non-Arrhenius behavior; namely, regions I to IV in fig. 2B have dramatically different slopes in plots of ln(rate) versus $1/T$. The additional increase in the etching rate above 850 K is due to evaporation of GaAs [8]. In the following three sections, MMBS, TPR and AES are used to show that this unusual surface temperature dependence of the steady state etching rate correlates with the surface chlorine coverage.

3.2. Modulated molecular beam scattering

In the MMBS experiments, the time scale for Cl_2 beam modulation was chosen so that steady state was achieved in each modulation cycle. For the GaAs/Cl_2 etching reaction over the temperature range of 350 to 800 K and for a Cl_2 flux of $\sim 7.5 \times 10^{14}$ molecules/cm^2/s (~ 1.2 monolayers (ML)/s, see section 2), the steady state requirement necessitates that the Cl_2 beam remains on for several seconds. In the experiments reported here, symmetric modulation cycles (equal on/off times) were employed. The cracking patterns for the various ions in each waveform were deconvoluted according to procedures previously described [8]. It is important to note here that since the time intervals over which the ion intensities are measured and stored in each bin of the multichannel scalar are large (~ 11 ms) compared with the differences in the measured velocity distributions (~ 100 μs [8]) the steady state mass fragmentation patterns determined in ref. [8] are valid. For convenience in discussing the product waveforms, we divide the temperature range studied into four regions as denoted in fig. 2. In regions I and III, the etching rate changes with surface temperature, and, as shown in figs. 3A and 3B, the modulation waveforms for the $GaCl_3$ and GaCl products show a slow exponential decay when the Cl_2 beam is off. The evolution of chlorinated products after the Cl_2 beam is turned off indicates that the surface is chlorinated at steady state. This behavior, as well as the changes in the steady state etching rate with surface temperature in these regimes, is characteristic of processes whose rates are surface reaction-limited. By contrast, in regions II and IV, the steady state etching rate is indepen-

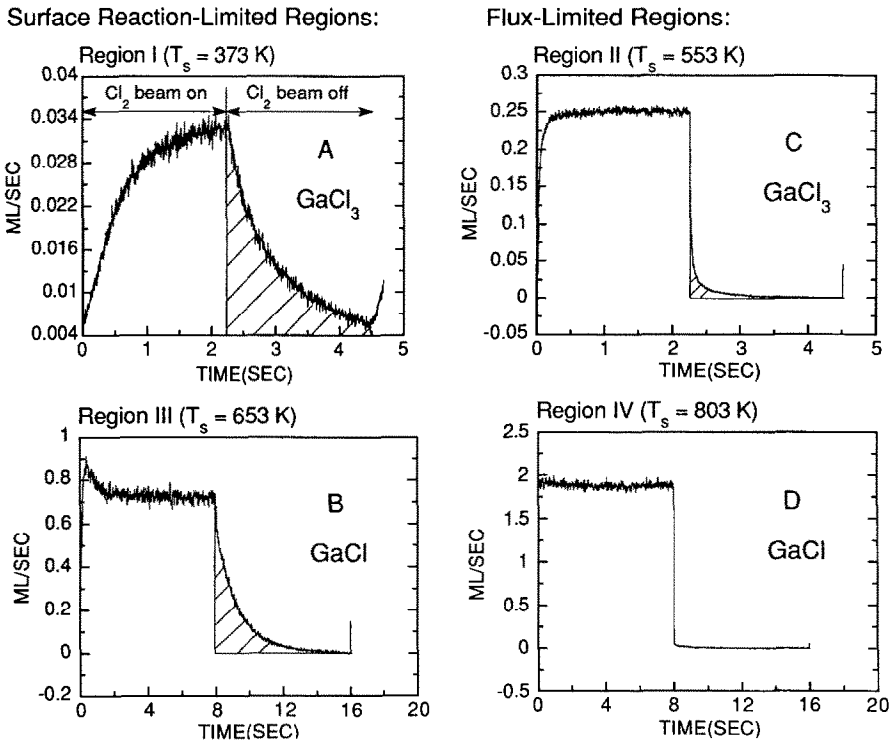

Fig. 3. Illustrative modulation waveforms for $GaCl_3$ and GaCl evolution from GaAs at the indicated temperatures. Regions I–IV refer to the temperature ranges labelled in fig. 2. The Cl_2 flux in these experiments was $\sim 7.5 \times 10^{14}$ Cl_2/cm^2/s, and the Cl_2 waveform was a square wave with periods of 4.5, 16, 4.5 and 16 s in (A) to (D), respectively. The slow decay of the $GaCl_3$/GaCl signal in (A) and (B) when the Cl_2 beam is off indicates that surface processes are rate-determining. The nearly square wave behavior for the product fluxes in (C) and (D) is characteristic of processes limited by the flux of Cl_2.

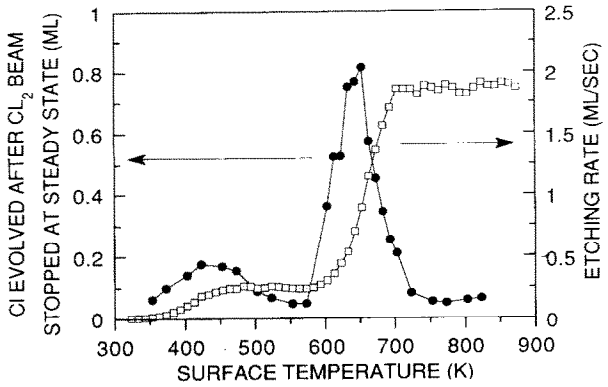

Fig. 4. Surface temperature dependence of the chlorine evolved after the Cl_2 beam is stopped at steady state. The evolved chlorine is determined from integration of the post-steady state transients in the MMBS waveforms (the shaded regions in fig. 3). For comparison, the square points show the surface temperature dependence of the steady state etching rate.

dent of surface temperature, and the modulation waveforms in figs. 3C and 3D are approximately square. In other words, the rates of $GaCl_3$ and GaCl evolution track directly with the Cl_2 modulation, which is characteristic of a flux-limited process.

By integrating the post-steady state transients in the MMBS waveforms of the chlorinated etching products, we can obtain information about the surface chlorine coverage at steady state. We must keep in mind, however, that only chloride products that desorb from the surface can be detected by MMBS. Hence, the "Cl coverage" established by this method is the Cl coverage relative to that which is stable on the surface in vacuum at the temperature of the experiment. We return to this point in section 4. The variation in the amount of Cl evolved in the MMBS experiments as a function of surface temperature (T_s) is plotted on fig. 4 (solid line). The values plotted represent the shaded areas in fig. 3 multiplied by the Cl/Ga stoichiometry of the products, i.e., 3 for $GaCl_3$ and 1 for GaCl. Also, included in these values are small contributions from $AsCl_3$ evolved at temperatures below 500 K. As discussed in section 2, the monolayer scales in figs. 3 and 4 were established by assuming that the maximum Cl coverage in the form of GaCl is 0.75 monolayers (ML) when the surface is saturated with chlorine at 550 K. In other words, we assume that the GaCl TPR peak area (see below) corresponds to a surface GaCl coverage of 0.75. For comparison, this calibration gives coverages and etch rates that are a factor of 2.35 smaller than those determined previously by comparing the ion intensities for GaAs evaporation with the absolute evaporation rate measured gravimetrically [8]. Both calibrations indicate that to within the experimental uncertainty the amount of Cl evolved is in the monolayer regime.

For purposes of comparison, the absolute etching rate (open squares) has also been plotted in fig. 4. Note that the two peaks observed for Cl evolution in the MMBS experiments occur at the same temperature where the etching rate increases with surface temperature. Thus, changes in the steady state etching rate are correlated with the evolution of chlorinated products in MMBS. Further discussion of the mechanistic implications of these results is deferred to section 4.

3.3. Temperature-programmed reaction

To investigate the nature and thermal stability of the chlorinated monolayer formed on GaAs, TPR experiments have been performed. In these studies, GaAs was exposed to a Cl_2 flux of 7.5×10^{14} molecules/cm^2/s for 1000 s at 340 K. This exposure saturates the surface with Cl_2. Temperature-programmed reaction spectra were recorded for fragments corresponding to Cl_2, $AsCl_x$ ($x = 1, 2$), $GaCl_x$ ($x = 1$–3) and As_x ($x = 2$–4). Here, we present only the results for the chlorinated products. The plots shown in fig. 5 are typical spectra obtained for (A) $GaCl_2^+$ and (B) $GaCl^+$. The relative intensities of all $GaCl_x$ species ($x = 1$–3), when compared to the cracking pattern of $GaCl_3$ [8], allow the two low temperature peaks (390 and 430 K) to be assigned as $GaCl_3$ ($GaCl_2^+$ is the base peak for $GaCl_3$ molecule), while the high temperature peak (600 K) is GaCl. The two distinct desorption temperatures as well as the evolution of two different chlorinated products indicate that at least two types of chlorinated species exist on the GaAs

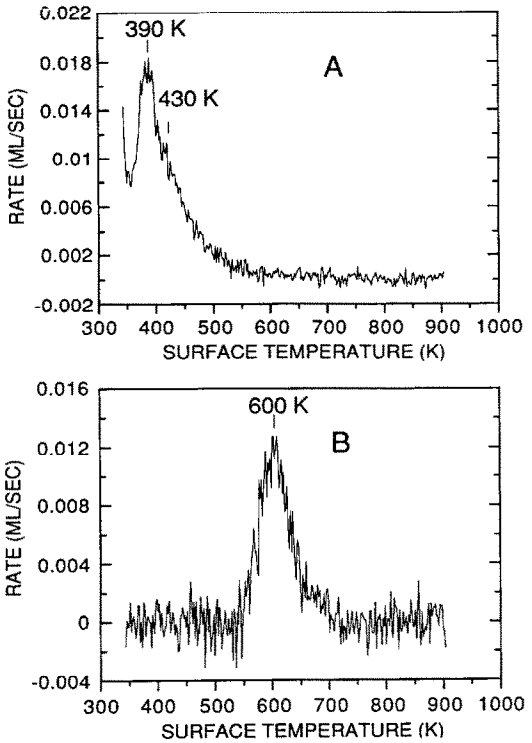

Fig. 5. Temperature-programmed reaction spectra for (A) $GaCl_3$ and (B) GaCl after saturating the surface with chlorine at 340 K. The surface heating rate is 1 K/s. The product evolution rates are normalized to a GaCl yield of 0.75 monolayer (1 monolayer (ML) = 6.25×10^{14} molecules/cm^2).

surface. As mentioned previously, the absolute product fluxes given on the TPR plots were obtained by assuming that the total area of the GaCl peak corresponds to $\theta_{GaCl} = 0.75$ (4.7×10^{14} molecules/cm^2). Note that $GaCl_3$ and GaCl evolution occur over the same temperature ranges where the steady state etching rate increases (fig. 2B). This result is consistent with the MMBS results for Cl evolution. The similarities in these three results are due in part to similar surface preparations. All three studies were performed on GaAs surfaces which were normally of (100) orientation but which had been roughened by extensive etching. The recent TPR results of Ludviksson et al. show that the spectra for GaAs(100)/Cl_2 depend on how the surface is prepared [24]. The surfaces here reflect those present during steady state etching.

No detectable $AsCl_x$ products were observed within the 350–850 K temperature range of these TPR experiments. This result is consistent with our finding in studies under UHV conditions (when the crystal could be cooled to 100 K) that $AsCl_3$ is evolved from GaAs at 180 K. $AsCl_3$ formation/desorption is therefore not the rate-determining step in the steady state etching of GaAs above room temperature.

3.4. Auger electron spectroscopy

Both the MMBS and TPR studies indicate that the steady state etching of GaAs with Cl_2 is correlated with the surface chlorine coverage and that this coverage is within the monolayer regime. These inferences are supported by AES measurements of the Cl coverage as a function of surface temperature. Since at least 15 s were required to scan the Cl AES peak, it was not feasible to perform AES measurements while linearly heating the sample at 1 K/s. As a result, the following procedures were used in order to investigate the effect of surface temperature on the chlorine coverage both with and without a flux of Cl_2 incident on the surface. For the vacuum experiments, the surface was exposed to 2 L of Cl_2 at 110 K, followed by flashing the sample to a temperature between 150 and 700 K. An AES spectrum was then recorded at 150 K. In order to minimize the electron stimulated desorption (ESD) effects, the AES spectrum was acquired only over the ^{181}Cl peak. The remaining Cl was then desorbed from the surface at 770 K followed by re-exposure at 110 K and heating to the next temperature. This procedure minimized the effects of Cl evolution during heating to the desired temperature. The results are shown as the open square points of fig. 6. Notice that as T_s increases from 200 K, the surface Cl concentration remains constant until T_s is above 280 K, the surface Cl concentration then decreases, reaching a plateau between 450 and 550 K, followed by a rapid decrease at higher temperature. Above 700 K, no Cl remains on the surface. This result is consistent with findings from XPS studies of GaAs(100)/Cl_2 [9].

The solid square points in fig. 6 are the ^{181}Cl AES peak intensities measured while the surface

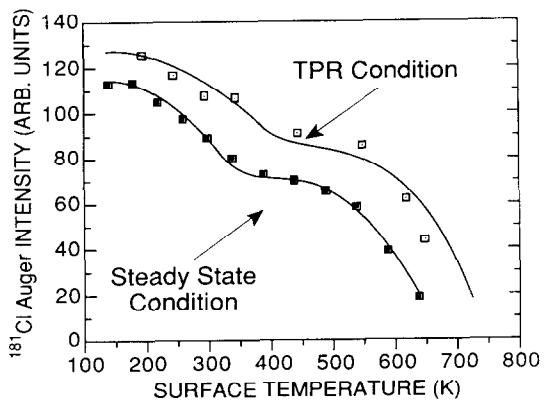

Fig. 6. AES studies of the Cl coverage on GaAs(100) as a function of surface temperature (T_s) under two different experimental conditions. The open square points were obtained by adsorbing 2 L of Cl at 110 K followed by flashing to the indicated T_s. The solid square points were obtained at steady state under a Cl_2 flux of $\sim 2\times10^{13}$ $Cl_2/cm^2/s$. The lines are shown as guides for the eye.

was etched continuously by Cl_2 molecules at a flux of 0.025 ML/s ($P_{Cl_2} = 1.4\times10^{-7}$ Torr). Compared to the results for the monolayer experiments above, it is clear that both curves follow the same trend with similar intensities. Based on the relative cross sections for the ^{181}Cl and ^{1070}Ga or ^{1228}As AES peaks [33], the maximum Cl signals in fig. 6 correspond to a Cl/Ga ratio of 0.3. Given the penetration depth of Auger electrons, this ratio is consistent with a surface Cl/Ga ratio in the monolayer regime. Note also that the change in the surface Cl coverage is opposite to the trend in the steady state etching rate with surface temperature (compare fig. 2B and 6). In summary, the surface Cl coverages in both the monolayer adsorption and steady state etching experiments are in the monolayer regime and have profiles as a function of surface temperature that are opposite to that for the steady state etching rate.

4. Discussion

4.1. Correlation between the surface chlorine coverage and the etching rate at steady state

The MMBS, TPR, and AES results presented above all establish that the surface temperature dependence of the steady state etching rate is inversely correlated with the surface chlorine coverage. In particular, over the temperature ranges where the etching rate increases, there is a local maximum in the Cl evolution (as $GaCl_3$ and GaCl) in the MMBS (fig. 4) and TPR (fig. 5) experiments. AES studies (fig. 6) confirm that the surface chlorine coverage decreases in proportion to the chlorinated products detected. Since the etching rate at steady state must be equal to the rate of Cl_2 uptake by the surface, these results suggest that the rate of Cl_2 adsorption is proportional to the number of vacant sites on the surface. Notice, in particular, that for surface temperatures (T_s) between 600 and 700 K, the chlorine coverage drops rapidly to zero, i.e., the chlorine vacancies on the surface increase rapidly to a maximum (fig. 6), and the steady state etching rate (related to the Cl_2 reaction probability) increases dramatically to a maximum (fig. 2B). By assigning the limits of the surface Cl coverage and the Cl_2 reaction probability values of 0 and 1, the fractional reaction probability can be directly correlated with the chlorine vacancy concentration (1 minus the fractional coverage of chlorine) as shown in fig. 7. While the agreement is not quantitative, the correlation is quite striking, suggesting a Langmuir adsorption model to account for the Cl_2 reaction probability.

4.2. Langmuir adsorption model for the steady state etching of GaAs by Cl_2

Since the rate of chlorine uptake at steady state is related (via the Cl stoichiometry in the etching products) to the steady state etching rate, the correlation between the steady state etching rate and the number of chlorine vacancies on the surface suggests the following expression for the rate of chlorine uptake:

$$\mathrm{Rate}^{\mathrm{ads}}_{\mathrm{Cl}_2} = \Phi s(1-\theta_{\mathrm{Cl}}), \qquad (1)$$

where Φ is the incident Cl_2 flux, s is the sticking probability on vacant sites, and θ_{Cl} is the fraction of surface sites occupied by chlorine. Such an expression is indicative of Langmuir adsorption kinetics, i.e., only chlorine molecules that strike empty surface sites are adsorbed. Note that by

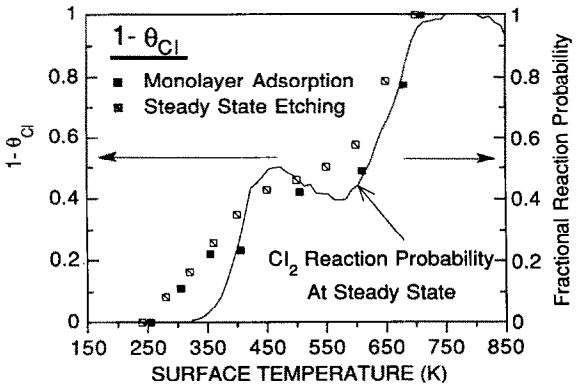

Fig. 7. Comparison of the surface temperature dependence of the normalized Cl_2 reaction probability and $1-\theta_{Cl}$ where the Cl_2 reaction probability is given by the non-reactively scattered Cl_2 signal from a steady state etching experiment (see ref. [8]) and θ_{Cl} is given by the ^{181}Cl Auger peak intensity normalized to 1 at 200 K (see fig. 6). The correlation between these two quantities suggests that the steady state etching rate is related to the number of vacant sites on the surface.

taking the adsorption probability to be proportional to $(1-\theta_{Cl})$ as suggested by the correlation in fig. 7, we have effectively assumed that only one vacant site is required for dissociative adsorption of Cl_2. While the documented role of a molecular precursor state for Cl_2 adsorption [2,3,6,34] will cause the precise expression for the adsorption probability to deviate from a strict $(1-\theta_{Cl})$ dependence, this functional form expresses the major features of the steady state etching behavior, and in the absence of a more accurate relation, a $(1-\theta_{Cl})$ dependence is assumed. For the rate of chlorine removal from the surface, we use:

$$\text{Rate}_{Cl}^{\text{removal}} = \alpha k \theta_{Cl}, \tag{2}$$

where α is the Cl/Ga or Cl/As stoichiometry of the product, k is the rate constant for chloride product formation/evolution, and the reaction rate is taken as first order in chlorine coverage. The first order dependence of the product evolution rate is consistent with the decay in the GaCl MMBS waveforms which can be reasonably fit by a single exponential. For $GaCl_3$, θ_{Cl} is a zeroth order approximation to a more complex coverage dependence. At steady state (SS), the rate of Cl_2 adsorption is half the rate of Cl removal, and the Cl coverage is therefore given by:

$$\theta_{Cl}^{SS} = 1/(1+\alpha k/2\Phi s). \tag{3}$$

This relation has the functional form shown by the bold lines in figs. 8A and 8B. At low temperatures the fractional chlorine coverage is ~ 1 but above a certain temperature, which is determined by the values of the rate constant (k) and the flux · sticking probability product (Φs), the coverage drops rapidly to zero. In the case of

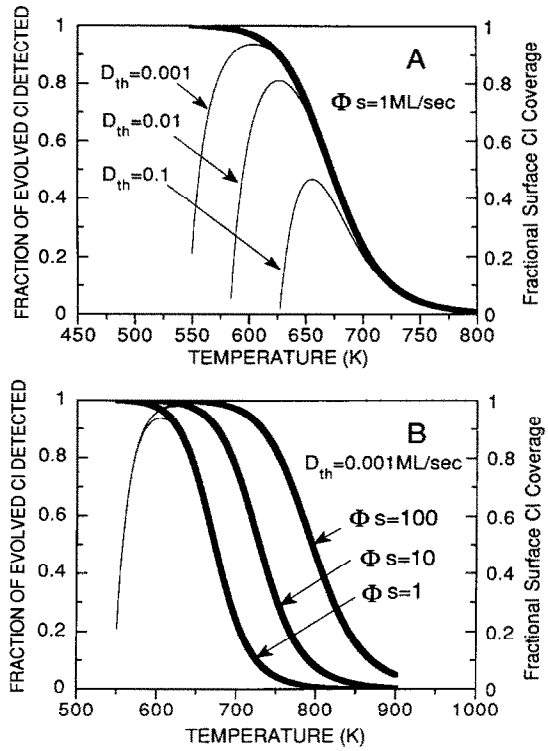

Fig. 8. The effects of Φs (flux·sticking probability) and D_{th} (detection threshold) on the amount of evolved chlorine detected in a modulated molecular beam scattering experiment. As described in the text, a Langmuir adsorption model has been utilized in deriving these curves. The bold lines show the actual chlorine surface coverage (right ordinate scale), while the thin lines show the amount of chlorine actually detected for the indicated parameters (left ordinate scale). In (A), Φs is fixed at 1 monolayer (ML)/s, while in (B) D_{th} is fixed at 0.001 ML/s. Notice that while the fractional surface coverage of Cl in each of these simulations was 1 at 500 K, the maximum amount of Cl detected depends on D_{th} and Φs and is significantly less than 1 if Φs is too small or D_{th} is too large.

Cl_2/GaAs, there are two such decreases in the surface chlorine coverage (fig. 6). These decreases correlate with the two different rate constants for Cl removal evidenced by the TPR results in fig. 5. Between 350 and 450 K, chlorine leaves the surface as $GaCl_3$ while between 550 and 650 K GaCl is evolved. In other words, there are two "states" for chlorine on the surface: a high coverage state which can form $GaCl_3$ at low temperatures and a low coverage state which must remain on the surface up to 550 K where GaCl is evolved. A possible molecular basis for this behavior will be discussed in section 4.5. In any event, the net result is that in order for eq. (3) to describe the chlorine coverage during GaAs etching, two coverage regimes with different chlorine evolution rate constants must be specified. In the sections below, these coverage regimes and rate constants, which can be determined from the *monolayer* AES and TPR results, are used to fit the modulated molecular beam scattering results determined at *steady state*.

4.3. Simulation of the modulated molecular beam scattering experiment

4.3.1. Effects of incident flux and detection threshold

Before applying the Langmuir model in section 4.2 to the MMBS results, the effects of the incident chlorine flux and the product detection threshold should be briefly addressed. Specifically, the integrated product yield is only proportional to the amount of chlorine evolved if the mass spectrometer has absolute detection sensitivity. The question we wish to address is: "How does the measured yield vary with the chlorine flux and mass spectrometer detection sensitivity?" To see this, consider the following. At the point where the rate of evolution of chlorinated products drops below the detection threshold (D_{th}, the minimum rate measurable), the chlorine coverage remaining on the surface is given by $D_{th}/\alpha k$. Thus, the amount of chlorine evolved *and* detected is proportional to the surface coverage at steady state (eq. (3)) minus $D_{th}/\alpha k$ (a proportionality constant is needed in eq. (4) to relate the flux entering the mass spectrometer to the total flux evolved from the surface with the assumption that the product angular distribution is the same for all products and experimental conditions):

$$\theta_{Cl}^{detected} \propto \frac{1}{1+\alpha k/2\Phi s} - \frac{D_{th}}{\alpha k}. \tag{4}$$

The way that the parameters in eq. (4) affect the MMBS results is illustrated in fig. 8 for $\alpha = 1$ and $k = \nu \exp(-E_a/kT)$ with $\nu = 10^{13}$ s^{-1} and $E_a = 40$ kcal/mol. The bold lines show the Cl coverage on the surface at steady state as given by the first term in eq. (4), while the fine lines show how the amount of Cl actually detected varies with the Cl_2 flux and sticking probability on vacant sites (Φs) and the detection threshold (D_{th}). Clearly, the surface temperature dependence of the Cl detected in MMBS is a sensitive function of these parameters. Of particular significance is the observation that if either D_{th} is too large or Φs is too small then the maximum amount of chlorine detected is substantially less than the actual surface coverage. With this point in mind, the experimental MMBS results in fig. 4 can now be fit to eq. (4). For the reasons mentioned in section 4.2, the low (< 550 K) and high (> 550 K) temperature etching regimes are considered separately below.

4.3.2. Etching at high temperature (550 K $< T_s <$ 850 K)

In this temperature range, the chlorinated product is GaCl. From the TPR results in fig. 5 and the MMBS results in fig. 3, the detection threshold for GaCl is estimated to be in the range of 0.005 to 0.02 ML/s. In addition, by assuming a first order pre-exponential factor (ν) of 10^{13} s^{-1} for GaCl evolution, we calculate [35] an activation energy (E_a) of 39 kcal/mol. Using $k = \nu \exp(-E_a/kT)$, we can now fit the MMBS data in fig. 4 to eq. (4) by adjusting Φs and D_{th}. In particular, by setting $\Phi s = 1.14$ ML/s and $D_{th} = 0.07$ ML/s, the fit shown in fig. 9A is obtained. Significantly, the value of Φs is within 5% of the Cl_2 flux (1.2 ML/s) determined by assuming that the GaCl TPR peak corresponds to $\theta_{GaCl} = 0.75$ (see the section 2), and the value of D_{th} is within a factor of 4 of that estimated. Smaller values of

D_{th} broaden the fit to lower temperature (see fig. 8A). The fact that the kinetic parameters for GaCl evolution from a chlorinated *monolayer* quantitatively reproduce both the peak temperature and width in the modulated steady state experiments strongly supports the Langmuir adsorption model and suggests that GaAs etching by chlorine at temperatures of 600–700 K is controlled by the rate of GaCl removal as has been previously suggested [9].

4.3.3. Etching at low temperature (350 K < T_s < 550 K)

The etching reaction in this lower temperature regime is analogous to that at higher temperatures in many respects. In both cases the increase in the steady state etching rate with surface temperature is correlated with the evolution of a gallium chloride product in TPR/MMBS and with a decrease in the chlorine AES peak intensity. The major differences at these lower temperatures are that (1) the increase in the etching rate correlates with the evolution of $GaCl_3$ as opposed to GaCl ($\alpha = 3$ as opposed to 1 in eqs. (2) and (3)), and (2) after all of the $GaCl_3$ has evolved, the surface is still covered with a significant amount of chlorine as opposed to the chlorine-free surface formed above 700 K. In addition, a single activation energy for $GaCl_3$ evolution does not provide a satisfactory fit to either the $GaCl_3$ TPR or MMBS results. While the TPR peak shape cannot be accurately determined because of the finite desorption rate at the adsorption temperature (see fig. 5), both the TPR and MMBS peaks are much broader than expected for a single activation energy and/or pre-exponential factor. Among the possible explanations for the broadness of these peaks are a coverage dependence of the activation energy or multiple surface sites (each with a different E_a for reaction). Either explanation can account for the results. For purposes of illustration, we choose a coverage-dependent activation energy to fit the results. In particular, we use the function $E_a + \lambda\theta$ where $E_a = 31$ kcal/mol, $\lambda = -4.4$ kcal/mol, and $\theta = 2.75 - T_s/200$ (a linear approximation for the temperature dependence of the surface chlorine coverage). This function produces a broadened

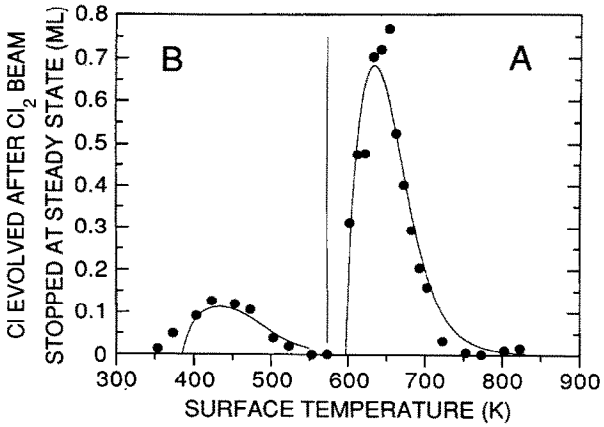

Fig. 9. Computer simulation based on the models described in the text for the amount of Cl detected in MMBS by integration of the post-steady state transients. The model parameters for (A) above 550 K and (B) below 550 K are given in the text. The dots are the experimental points from fig. 4; for purposes of comparison, the minimum measured value has been set to zero.

TPR peak, consistent with the $GaCl_3$ TPR results in fig. 5. Taking Φs to be 1.14 ML/s (the same value that gives a best fit to the high temperature results) and using a detection threshold of 0.0015 ML/s (consistent with the MMBS and TPR results) the fit shown in fig. 9B is obtained when the first term in eq. (4) is multiplied by 0.13 [36]. Having previously found evidence that $GaCl_3$ formation may occur at surface defects, this multiplicative constant can be interpreted as the fractional coverage of defect sites on the surface. Such a value is reasonable based on the degree of surface roughness observed in electron and tunneling microscopy studies of etched wafers [8]. While more quantitatively accurate fits to the data in fig. 9 can be obtained by further refinement of the parameters above, the resulting parameters are substantially outside the ranges estimated for the variables. The point we wish to make is that by using parameters in the Langmuir model that are all physically reasonable based on independent experiments and calculations, the model yields an extremely good fit to the experimental MMBS results as shown by the curves in fig. 9.

4.4. Limitations of the model

While the correlation between the Cl_2 reaction probability and $(1-\theta_{Cl})$ strongly supports a Langmuir-type adsorption model for the Cl_2 etching of GaAs, a strict $(1-\theta_{Cl})$ dependence for the Cl_2 adsorption probability is too simple to account for the more subtle features of the etching reaction. A particularly notable simplication is the assumption that the dissociative sticking probability, s, on an empty surface site is constant. As recently demonstrated in an series of elegant angle-resolved molecular beam scattering (MBS) experiments by DeLouise, this assumption ignores the dynamical effects of trapping and desorption from a molecular precursor state on the Cl_2 dissociation probability [3]. Indeed, there is clear evidence for a molecular precursor at temperatures below 500 K [3], and, as DeLouise notes, competition between dissociation and desorption from the precursor state can account, at least in part, for the local maximum in the Cl_2 reaction probability reported by some investigators [1,3]. Based on our findings here on the surface Cl coverage, this precursor is probably an extrinsic precursor, i.e., exists on top of the Cl-covered surface sites.

4.5. A molecular explanation for the Langmuir model

In the Langmuir adsorption model presented above for the steady state etching kinetics no assumptions were made regarding the identity of the chlorinated surface species or the mechanisms by which the volatile chlorinated products are formed. While there is still controversy over whether Cl bonds to Ga and/or As on GaAs surfaces, recent results by Ludviksson et al. [24] suggest that, on a defect-free Gallium-rich c(8 × 2) GaAs(100) surface, Cl binds to Ga as a monochloride species, but $GaCl_2$ species can also be isolated at low temperatures on more As-rich surfaces. Based on these results, we propose that GaCl and $GaCl_2$ are the chlorinated surface species during steady state etching of GaAs(100). In this picture, GaCl desorption at 550–650 K produces $GaCl_{(g)}$ while $GaCl_2$ disproportionation produces $GaCl_3$ (which desorbs) and GaCl (which remains adsorbed at temperatures below 550 K). Since there is insufficient space for all surface Ga atoms on (100) terraces to accommodate two chlorine atoms, it is possible that this kind of disproportionation reaction occurs only at edge positions, i.e., defect sites, as the low temperature simulation in section 4.3 suggests. Over the temperature range of 350 to 450 K where the etching rate is increasing to become flux-limited, the chlorine monolayer on the surface is converting from $GaCl_2$ to GaCl. Some partially chlorinated arsenic species must also be present based on the evolution of some $AsCl_3$ (see fig. 2). The etching rate again increases above 550 K where GaCl desorbs, and the surface monolayer changes from GaCl to a Cl-free surface.

In this picture, the Langmuir model for the non-Arrhenius behavior of the steady state etching of GaAs by Cl_2 (see fig. 2) is attributable, at a molecular level, to the instability of $GaCl_2$ with respect to GaCl formation if there are vacant Ga sites on the surface. Only when the monolayer is saturated with GaCl can $GaCl_2$ form and produce $GaCl_3$. Specifically, for high surface Cl coverages where $GaCl_2$ exists on the surface, $GaCl_3$ is formed and evolved at temperatures as low as 350 K; a GaCl monolayer, on the other hand, is stable with respect to forming $GaCl_2$ and $GaCl_3$. Although there is abundant chlorine on the surface in this GaCl monolayer, the chlorine does not diffuse together to form $GaCl_3$, even when the surface temperature is 100–200 K above where $GaCl_3$ is evolved from a highly chlorinated surface (see fig. 5). Such behavior is typical of adsorbates on semiconductor surfaces. For example, high coverages of hydrogen on silicon surfaces form a dihydride phase which desorbs as H_2 at 670 K leaving behind a monohydride state which also evolves as H_2 but at 780 K [37]. It has been suggested that this difference in the two desorption temperatures reflects an instability of the dihydride with respect to the monohydride when there are unoccupied silicon atoms [38]. In the case of GaAs/Cl, the impact of this higher chloride/lower chloride equilibrium on the steady state etching rate is non-Arrhenius behavior: $GaCl_2$ reacts to evolve $GaCl_3$ at low surface

temperatures but the etching rate plateaus above 500 K (for the flux used here) where the $GaCl_3$ formation rate catches up with the Cl_2 flux and the surface stoichiometry becomes GaCl. The etching rate is then flux-limited until above 550 K where GaCl is evolved. Finally, above 700 K, the process is again flux-limited where the surface is essentially chlorine-free.

5. Conclusions

By combining the results from monolayer adsorption experiments under UHV conditions with molecular beam scattering studies of the reaction at steady state, we have demonstrated that the rate at which Cl_2 etches GaAs is approximately proportional to $(1 - \theta_{Cl})$, i.e., the number of vacant sites on the surface. A Langmuir adsorption model that incorporates kinetic parameters from *monolayer* temperature-programmed reaction experiments quantitatively reproduces the results from modulated molecular beam scattering studies of the *steady state* etching reaction. The results also suggest a molecular-level explanation for the non-Arrhenius surface temperature dependence of the steady state etching rate.

Acknowledgements

Financial support from the donors of the Petroleum Research Fund Administered by the American Chemical Society (ACS-PRF 22978-AC5) is gratefully acknowledged. B.E.B. and M.F.V. gratefully acknowledge support from the National Science Foundation (DMR 89-57236 and CHE85-5277) as Presidential Young Investigators.

References

[1] M. Balooch, D.R. Olander and W.J. Siekhaus, J. Vac. Sci. Technol. B 4 (1986) 794.
[2] L.A. DeLouise, J. Chem. Phys. 94 (1991) 1528.
[3] L.A. DeLouise, J. Vac. Sci. Technol. A 9 (1991) 1732.
[4] L.A. DeLouise, J. Appl. Phys. 70 (1991) 1718.
[5] N. Furuhata, H. Miyamoto, A. Okamoto and K. Ohata, J. Appl. Phys. 65 (1989) 168.
[6] L.A. DeLouise, Surf. Sci. Lett. 244 (1991) L87.
[7] H. Hou, Z. Zhang, S. Chen, C. Su, W. Yan and M. Vernon, Appl. Phys. Lett. 55 (1989) 801.
[8] C. Su, H. Hou, Z.G. Dai, G.H. Lee, M. Vernon and B. Bent, J. Vac. Sci. Technol., submitted.
[9] C.L. French, W.S. Balch and J.S. Foord, J. Phys.: Condensed Matter 3 (1991) S351.
[10] V. Liberman, G. Haase and R.M. Osgood Jr., Chem. Phys. Lett. 176 (1991) 379.
[11] D. Troost, L. Koenders, L.Y. Fan and W. Mönch, J. Vac. Sci. Technol. B 5 (1987) 1119.
[12] J.H. Ha, E.A. Ogryzlo and S. Polyhronopoulos, J. Chem. Phys. 89 (1988) 2844.
[13] N. Furuhata, H. Miyamoto, A. Okamoto and K. Ohata, J. Electron. Mater. 19 (1990) 201.
[14] A. Freedman and C.D. Stinespring, Mater. Res. Soc. Symp. Proc. 158 (1990) 389.
[15] R.B. Jackman, G.C. Tyrrell, D. Marshall, C.L. French and J.S. Foord, Mater. Res. Soc. Symp. Proc. 223 (1991) 215.
[16] M.S. Ameen and T.M. Mayer, J. Appl. Phys. 63 (1988) 1152.
[17] W.L. O'Brien, C.M. Paulsen-Boaz and T.N. Rhodin, J. Appl. Phys. 64 (1981) 6523.
[18] R.J. Davis and E.D. Wolf, J. Vac. Sci. Technol. B 8 (1990) 1798.
[19] S.M. Mokler, P.R. Watson, L. Ungier and J.R. Arthur, J. Vac. Sci. Technol. B 8 (1990) 1109.
[20] S.M. Mokler and P.R. Watson, Solid State Commun. 70 (1989) 415.
[21] C.I.H. Ashby, Appl. Phys. Lett. 45 (1984) 892.
[22] Q.Z. Qin, Y.L. Li, Z.K. Jin, Z.J. Zhang, Y.Y. Yang, Z.H. Cai, X.N. Liu, Z.G. Dai, W.J. Jia and Q.K. Zheng, Sci. China 33 (1990) 607.
[23] R.D. Schnell, D. Rieger, A. Bogen, K. Wandelt and W. Steinmann, Solid State Commun. 53 (1985) 205.
[24] A. Ludviksson, M. Xu and R.M. Martin, Surf. Sci. 277 (1992) 282.
[25] A. Freedman and C.D. Stinespring, J. Phys. Chem. 96 (1992) 2253.
[26] G. Margaritondo, J.E. Rowe, C.M. Bertoni, C. Calandra and F. Manghi, Phys. Rev. B 22 (1981) 509.
[27] C. Sasaoka, Y. Kato and A. Usui, Jpn J. Appl. Phys. 30 (1991) L1756.
[28] C. Su, Z.G. Dai, G.H. Lee and M. Vernon, Mater. Res. Soc. Symp. Proc. 204 (1991) 31.
[29] D.R. Miller, in: Atomic and Molecular Beam Methods, Vol. 1, Ed. G. Scoles (Oxford University Press, New York, 1988) p. 14.
[30] C.T. Foxon, J.A. Harvey and B.A. Joyce, J. Phys. Chem. Solids 34 (1973) 1693.
[31] C.T. Foxon, B.A. Joyce, R.F.C. Farrow and R.M. Griffths, J. Phys. D: Appl. Phys. 7 (1974) 2422.
[32] C.M. Chiang, T.H. Wentzlaff and B.E. Bent, J. Phys. Chem. 96 (1992) 1836.

[33] S. Mroczkowski and D. Lichtman, J. Vac. Sci. Technol. A 3 (1985) 1860.
[34] L.A. DeLouise, Chem. Phys. Lett. 180 (1991) 149.
[35] P.A. Redhead, Vacuum 12 (1962) 203.
[36] The substantially lower detection sensitivity for GaCl compared with $GaCl_3$ (see ref. [8]) is attributable to the ionization cross section (ref. [8]) and a higher background in the mass spectrometer at $m/e = 110$ ($GaCl^+$) than at $m/e = 141$ ($GaCl_2^+$).
[37] R. Imbihl, J.E. Demuth, S.M. Gates and B.A. Scott, Phys. Rev. B 39 (1989) 5222, and references therein.
[38] S.F. Shane, K.W. Kolasinski and R.N. Zare, J. Chem. Phys. 97 (1992) 3704.